

## INFLUENCE OF THE ULTRASONIC ACTIVATION ON THE SOLDERING PROCESS OF COPPER BY USING Sn-Ag3.5% SOLDER

Sorin Vasile SAVU<sup>1</sup>, Ionel Danut SAVU<sup>2</sup>

*The paper presents analysis of the wetting process and nucleation and growing of the Ag<sub>3</sub>Sn intermetallic compound, when use Sn-Ag3.5% solder and resistive-ultrasonic hybrid heat source. The energy to the surface was calculated by using the viscosity of the solder, the Gruneisen factor, the frequency and the amplitude of the ultrasonic vibration. By using the RH method, it was measured the viscosity of the solder. By using specific model, it was calculated the surface tension of the solder on the substrate/pad. By experimental research it has been revealed an increasing of 2.5 times of the wetting for the hybrid heating, important susceptibility to cracking for the classic resistive heating and tin dioxides on the surface.*

**Keywords:** intermetallics compounds; nucleation and growth; bonding; ultrasonic processing; microstructure; MEMS

### 1. Introduction

The application of the Directive 2002/95/EC of the European Parliament forced the electronics producers to replace the content of lead with one or more elements in the tin alloy, in the condition of keeping low melting temperature of the new solder. The replacement brought two distinct problems to the soldering process: the new solders proved lower wetting capacity and nucleation and growth of specific intermetallic compounds (IMCs) which modifies the mechanical characteristics of the joint [1-7]. Improvement of the wetting is possible by adding different elements or by applying ultrasonic vibration. Galleguillos and Osorio [8,9] obtained a linearly dependency between the wetting capacity and the vibration velocity. In the same time, they showed that the wetting capacity is independent of the vibration frequency. The influence of the ultrasounds on the materials was studied by Zhu, who concluded that the thermodynamic properties of the materials are influenced by the ultrasonic field [10]. The application of an ultrasonic field on a molten metal is not very simple, due to the cavitation phenomenon which is specific to such interaction and it produces very thin bubbles which transfer to the molten

<sup>1</sup> Assoc. Prof., Dept. IMST, University of Craiova, Romania, e-mail: sorin.savu@yahoo.com

<sup>2</sup> Assoc. Prof., Dept. IMST, University of Craiova, Romania, e-mail: danut.savu@ymail.com

metal important quantity of energy by implosion [11].

According to Abtew [12] and Harris [3] using lead-free solder in which the lead was replaced with silver and/or silver plus copper additions, then  $\text{Cu}_3\text{Sn}$ ,  $\text{Cu}_6\text{Sn}_5$  and  $\text{Ag}_3\text{Sn}$  IMCs are formed during heating, aging and cooling processes which are specific to a soldering thermal cycle.

The paper presents two distinct researches: a theoretical and experimental study of the influence of the ultrasonic field on the wetting capacity of the solder and an experimental study on the nucleation and growth of the  $\text{Ag}_3\text{Sn}$  IMC when use Sn-Ag3.5% solder on copper base metal (substrate).

## 2. Influence of the ultrasonic activation on the wetting

According to the primary physics the wetting property is influenced by the surface tension of the liquid material. The surface tension is produced by the energies which are acting on the surface of the liquid. The same theory is valid for the molten solder, during the soldering process, when it is expected that the solder to have as high as possible wetting capacity. Starting with these considerations an analysis of the energies on the surface layer of the molten Sn-Ag3.5% solder is necessary. Solder atoms (mostly tin) from the surface layer produce the internal pressure. The mechanical work,  $W_{s,f}$ , realized by the surface forces influences the surface layer dimensions. The same mechanical work is considered negative (as sign) because the surface forces are acting in opposite direction comparing to the movement of the atoms from the surface layer:

$$W_{s,f} = -\gamma \cdot \Delta A_s \quad (1)$$

where  $\gamma$  is the surface tension coefficient of the solder and  $\Delta A_s$  is the solder surface layer area.

The value of the produced mechanical work is a measure of the surface layer energy which is created by the continuous impact between the atoms of the surface layer and the atoms of the vapors from the close neighborhood and that is a potential energy:

$$E_{s,p} = -W_{s,f} \rightarrow E_{s,p} = -(-\gamma \cdot \Delta A_s) \quad (2)$$

To that potential energy a new component is added by the mechanical ultrasonic vibration,  $E_{s,us}$ , but in the same time the ultra-acoustic energy is composed of potential energy  $E_{us,p} = \frac{1}{2} \cdot k \cdot p^2$  and kinetic energy  $E_{us,k} = \frac{1}{2} \cdot \rho \cdot v^2$ , where  $k$  is the compressibility of the molten surface layer  $p$  is the acoustic pressure (60 dB),  $\rho$  is the density of the molten solder ( $6.99 \text{ g/cm}^3$ ) and  $v$  is the energized particle velocity within the molten solder. The total energy to the surface layer becomes:

$$E_{s\_total} = \gamma \cdot \Delta A_s + \frac{1}{2} \cdot k \cdot p^2 + \frac{1}{2} \cdot \rho \cdot v^2 \quad (3)$$

It should be taken account that the absorption of ultrasound by the molten solder depends on the viscosity of the liquid solder, on the metal temperature, and on the thermal conductivity of the liquid solder. The velocity is determined by the frequency multiplied by the amplitude of the vibration,  $v = f \cdot A$ . Results:

$$\Delta A_s = \frac{1}{v} \cdot \left( E_{s\_total} - \frac{1}{2} \cdot k \cdot p^2 - \frac{1}{2} \cdot \rho \cdot f^2 \cdot A^2 \right) \quad (4)$$

All terms can be technologically defined, measured or analytical determined and due to that the extension or contraction of the surface layer can be evaluated. If  $\Delta A_s > 0$ , then a contraction of the surface layer will take place. If  $\Delta A_s < 0$ , then an extension of the surface will take place and that means a better wetting of the surface by the molten solder. In this case it can be considered that a better wetting will be recorded when

$$E_{s\_total} < \frac{1}{2} \cdot k \cdot p^2 + \frac{1}{2} \cdot \rho \cdot f^2 \cdot A^2 \quad (5)$$

where  $f$  is the frequency of the ultrasonic vibration (50kHz) and  $A$  is the amplitude of the vibration, set to 120  $\mu\text{m}$ .  $E_{s\_total}$  can be approximated by considering the natural energy of the surface (without the energetic activation by ultrasonic vibration), for a specific surface layer dimension  $\Delta A$  of the molten solder which has  $\gamma$  viscosity. Because the soldering process starts usually at 300 K and ends around 600 K, all the calculations and experimental determinations will cover these two temperatures. The determinations were done experimentally by using volume of 5.5  $\text{mm}^3$  (25 mm length / 0.7 mm diameter wire solder) and it was revealed that the Sn-Ag3.5% solder has 1.9  $\text{mPa}\cdot\text{s}$  viscosity to 600 K and 3.1  $\text{mPa}\cdot\text{s}$  to 400 K. Viscosity of the Sn-Ag3.5% solder as a function of temperature using the Robert Hammerle's method (by using a piezoelectric element energized to exhibit thickness-shear mode vibration) is presented in Fig. 2.



Fig. 1 Sn-Ag3.5% wire solder used for the calculation and for the experimental program

The compressibility factor is difficult to be experimentally determined, but there is a possibility to be calculated using the Gruneisen constant which is factor not dependent on the temperature. Contacted, the producer of the solder wire

specified 12.11 for 600 K value for the Gruneissen factor.

$$k = \frac{\alpha \cdot V}{\gamma \cdot c_V} \quad (6)$$

where  $\alpha$  is the thermal expansion coefficient (22.7  $\mu\text{m}/(\text{m}\cdot\text{K})$  at 300 K),  $V$  is the volume of the molten solder (5.5  $\text{mm}^3$ ),  $\gamma$  is the Gruneisen constant (12.11) and  $c_V$  is the specific heat at constant volume (227  $\text{J}/\text{kg}\cdot\text{K}$ ).

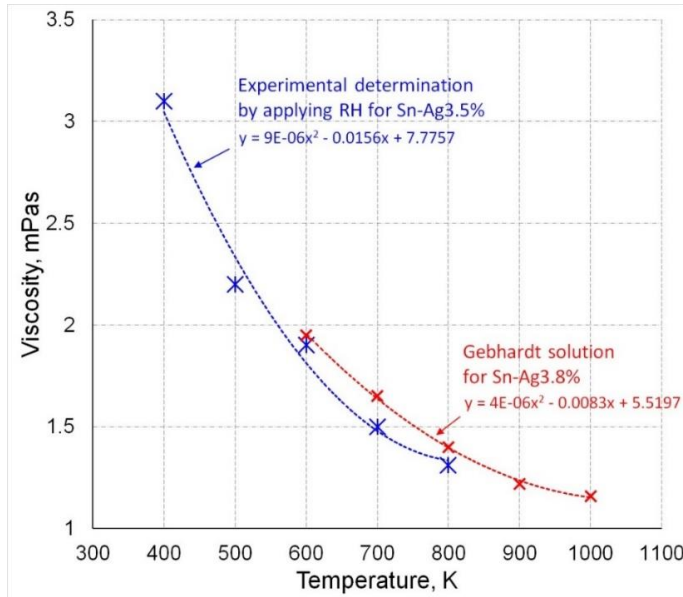


Fig. 2 Determined viscosity of the Sn-Ag3.5% solder and confirmation by comparing to values reported by Gebhardt [13]

The compressibility factor of the solder becomes 0.044 for 300 K and 0.0461 for 600 K. Calculated surface layer area was  $\Delta A_s = 18.78 \text{ mm}^2$ . Using the factors in the calculation of the surface layer energy without ultrasonic activation, it can be obtained:  $E_{s,1} = 0.044 \cdot 18.78 = 0.82 \text{ W}$ . In the same time, the energy brought locally by the ultrasonic vibration to the surface layer is:  $E_{s,US} = \frac{1}{2} \cdot 0.044 \cdot 6^2 + \frac{1}{2} \cdot 6.99 \cdot 50^2 \cdot 0.012^2 = 1.24 \text{ W}$ . The result shows an increasing of the wetting of about 2.5 times, which means important improving of conditions for the soldering process brought by the ultrasonic activation. The surface tension of the solder calculated according to the presented method is presented in Fig. 3.

Verification of the calculated result was experimentally done. Two identical volumes of solder were heated up to 600 K: the first by using resistive heating source only, without ultrasonic activation and the second one using hybrid source resistive in conjunction with ultrasonic vibration.

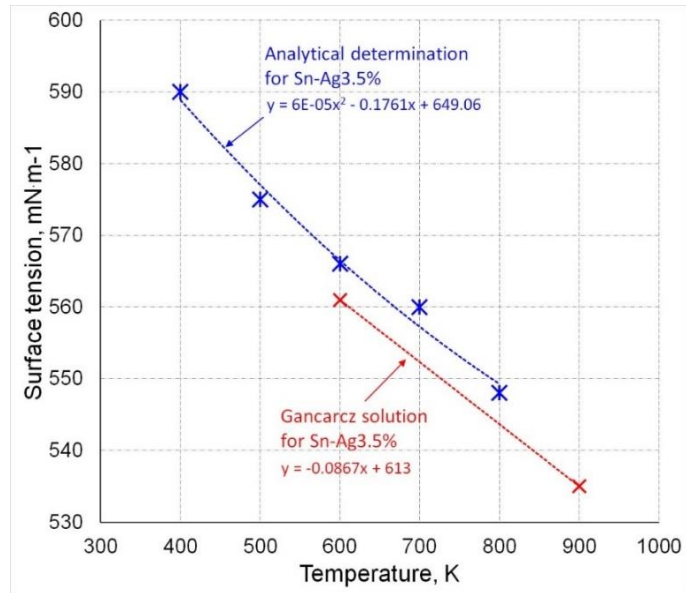


Fig. 3 Calculated surface tension of the Sn-Ag3.5% solder and confirmation by comparing to values reported by Gancarcz [13]

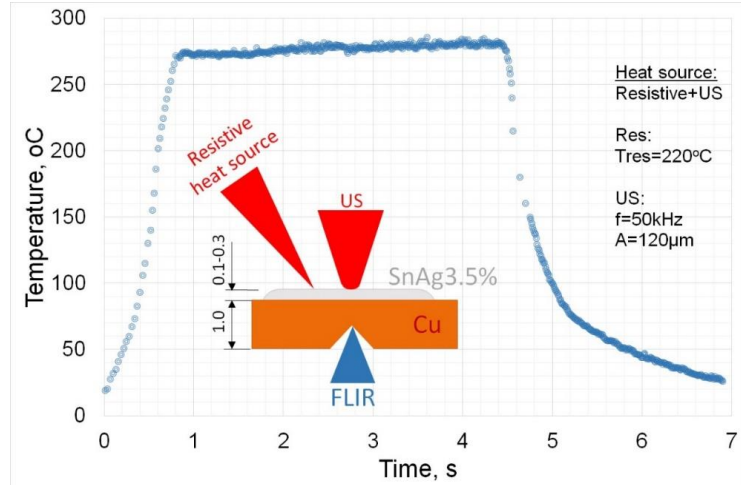


Fig. 4 Hybrid heating of the solder

For the experimental program as for the calculation it was used common solder wire: Sn-Ag3.5% lead free no clean core flux solder wire, having 3.5 +/- 0.2 silver and rest tin, according to EN-ISO 9453 and JIS Z 3282: 2006.

The properties of the used wire, according to the producer are: melting temperature - 221°C, coefficient of thermal expansion - 22.7  $\mu\text{m}/\text{m}^\circ\text{C}$  and density 7.36 g/ml. The resulted wetting (Fig. 6 a and b) was measured and compared. In the first case the wetting was on 18.25  $\text{mm}^2$  and in the second case the wetting

was on  $31.64 \text{ mm}^2$  (values obtained by USB microscope measurements).



Fig. 5 Experimental setup

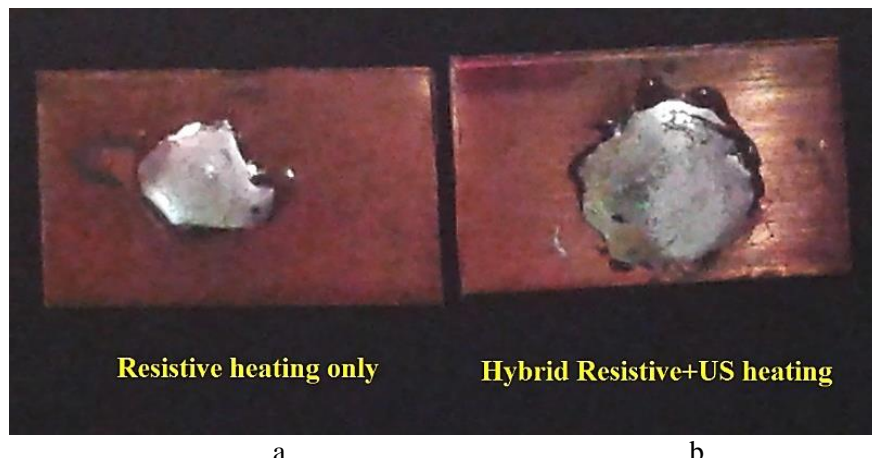


Fig. 6 Deposited solder with specific wetting (a. classic resistive heating and b. hybrid resistive and ultrasonic heating)

That means an increasing of 1.73 times which is lower than the calculated 2.5. The error comes in the experiment where it was difficult to maintain the horn of the sonotrode on the surface layer to transmit the energy in that layer. The

surface layer has atomic thickness and the horn entered deeper which means a transfer of energy to the core of the molten solder but to the surface layer. The loss of energy gave the main difference between the 2.5 and 1.73. The experiment was considered for 500K, 550K, 650K and 700K and the results of the wetting extension is presented in Fig. 7.

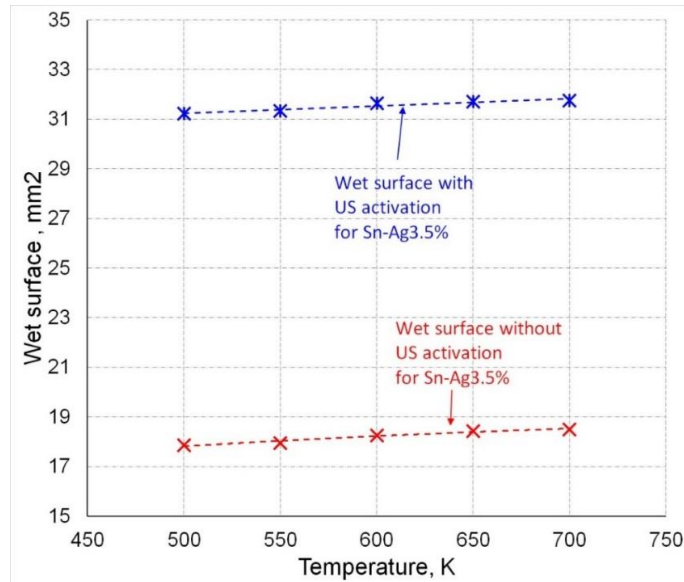


Fig. 7 The wet surfaces for the two versions of heating solder

The increased wetting of the solder influenced phenomenon observed for high kinetic undercooling: susceptibility to cracking of the deposited solder (Fig. 8).



Fig. 8 Deposited solder by classic resistive heating (medium wetting, susceptibility to cracking and high area of the surface layer covered by tin dioxide)

Fast cooling of the solder and its tendency to become spheroidal produce cracks on the surface, within the marginal areas where cooling is accelerated due to low thickness. The cracks are solidification cracks and they are positioned parallel to the solidification line.

Up to 1 mm opening to the surface the cracks are developing down to the interface base metal-solder. The initiation and the propagation of the cracks is lower when the wetting is increased by the ultrasonic activation. The cracking development was recorded to be in parallel with an important oxidation of the surface and the rutile tetragonal formed tin dioxide creates proper conditions for the cracking to initiate.

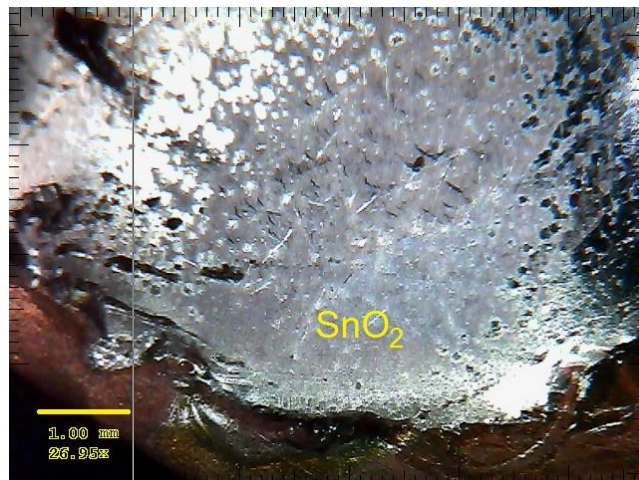


Fig. 9 Deposited solder by hybrid resistive plus ultrasonic heating (high wetting, low susceptibility to cracking and less than half area of the surface layer covered by tin dioxide)

A second observation is related to the surface covered by the tin dioxide. In the classic melting of the solder, using resistive heating source only, the tin dioxide covers more than 80% of the surface, which is almost double comparing to the hybrid heating (resistive and ultrasonic) where less than 40% of the surface is covered by the oxide.

### 3. Influence of the ultrasonic activation on the Ag<sub>3</sub>Sn IMC growth

Heating-cooling cycle specific to the soldering process creates liquid-solid interface between the solder and the base metal. The surface of the base metal is heated over 221°C (melting point of the solder), and metallurgical interaction at the interface is initiated. First, diffusion of atoms from the surface of the base metal to the molten solder is promoted and it increases with the soldering procedure parameters: temperature and time [15]. The migration of the atoms to the solder results in the formation of intermetallic compounds (IMCs). The

increasing of the wetting, according to the mechanism described above, means higher interface solid-liquid and higher potential for the IMCs to nucleate inside the deposited solder. Generally, the IMCs are high strength and high hardness phases and their nucleation and growth during and after the soldering process modify the characteristics of the material. Being brittle, the IMCs reduce the mechanical properties of the soldering joints and, subsequently, their lives [16.17]. When use SnAg3.5% solder on copper base metal,  $\text{Ag}_3\text{Sn}$  and  $\text{Cu}_3\text{Sn}$  IMCs start to nucleate and to grow-up inside the bond material [18]. Because  $\text{Cu}_3\text{Sn}$  IMC require 3 atoms of copper for 1 atom of tin, such IMC nucleates in the very near vicinity of the solid-liquid interface.  $\text{Cu}_3\text{Sn}$  forms a 3-6  $\mu\text{m}$  border along the interface and it captivates most of the diffused copper atoms. The atoms which received high energy from the heating source are able to migrate on higher distances and in the places where agglomeration of copper atoms is happening a new IMC is possible to be formed:  $\text{Cu}_6\text{Sn}_5$ . [3,19] When use SnAg3.5% solder the quantity of the formed  $\text{Cu}_6\text{Sn}_5$  is very low, almost negligible. The  $\text{Cu}_3\text{Sn}$  border is thinner comparing to the situation of using Sn-Ag-Cu solders, but the most important is the  $\text{Ag}_3\text{Sn}$  IMC.  $\text{Ag}_3\text{Sn}$  was revealed to have two types of shapes which appear on distinct cooling rates: flat islands in the matrix of  $\beta\text{-Sn}$  when the cooling rate is low and high dimension needles when the cooling rate is high (becoming small as particles when the cooling rate has very high values). [20-23]. When apply heating-cooling cycle specific to a soldering process, the cooling rate is high enough to obtain needle  $\text{Ag}_3\text{Sn}$  IMC. Being long and thin and brittle, the susceptibility to cracking of the joint increases with the volume of the formed  $\text{Ag}_3\text{Sn}$  IMC. The expertise we gained in analyzing the behavior of  $\text{Cu}_6\text{Sn}_5$  during ultrasonic energetic activation gives the possibility to propose similar activation of the molten solder and to record the growing process of the  $\text{Ag}_3\text{Sn}$  IMC. Experimental program was developed to understand the influence of the energetic activation by ultrasonic vibration of the molten solder on the growing process of the  $\text{Ag}_3\text{Sn}$ . Similar specimens to those created to analyze the viscosity of the solder were produced in the following conditions: specimen A done by using resistive classic soldering process, without energetic activation, and specimen B done by using hybrid (resistive and ultrasonic) heat source. The energetic activation was meant to introduce vibration [24-27] within the molten and solidified solder which was expected to result in a decreasing of the formed  $\text{Ag}_3\text{Sn}$  volume. The base metal was copper 0.5 mm thickness plate and the solder was SnAg3.5% solder wire having 0.7 mm diameter. Soldering parameters were: for specimen A – temperature  $T_{\text{sold res A}} = 260^\circ\text{C}$ , time  $t_{\text{sold A}} = 12\text{ s}$ , for specimen B – temperature  $T_{\text{sold res B}} = 240^\circ\text{C}$ , time  $t_{\text{sold B}} = 12\text{ s}$ ,  $f_{\text{sold B}} = 50,000\text{ Hz}$ ,  $A_{\text{sold B}} = 120\text{ }\mu\text{m}$ ,  $t_{\text{vib post-process B}} = 5\text{ s}$ . In the B process the ultrasonic vibration has been maintained 5 s after the ending of the hybrid heating, in order to influence the growing of the  $\text{Ag}_3\text{Sn}$ . The thermal cycles for the

two processes are presented in Fig. 10.

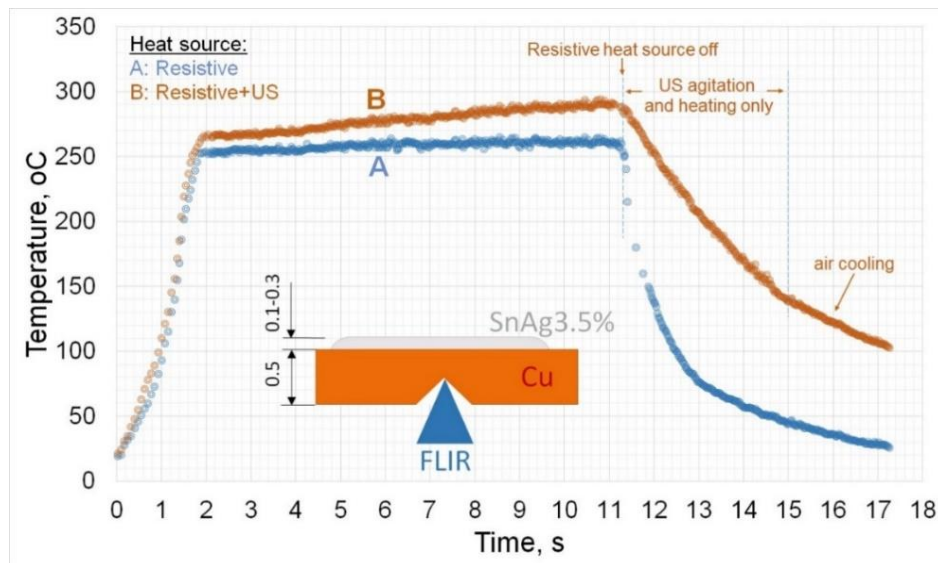


Fig. 10 Thermal cycles for the both versions of heating solder

The solder was deposited on the copper substrate and SEM analysis have been applied to the solder and the interface between the two metals. Specimen A presented rare but long  $\text{Ag}_3\text{Sn}$  needles, which was different from the specimen B where the number of the formations was higher, but the dimensions of the  $\text{Ag}_3\text{Sn}$  were at least 50% lower and breaking of the formed IMCs can be observed. Analysis of the specimen A revealed two situations: a. single nucleation of  $\text{Ag}_3\text{Sn}$  which grows up to the final dimension, and b. multiple local nucleation of  $\text{Ag}_3\text{Sn}$  which grow in time until joining together and producing single long needle. The nature of the IMC was proved by XRD analysis of the produced phases.

Fig. 11 is example of the recorded Thomson scattering against the diffraction Bragg angle  $2\theta$  in area where  $\text{Ag}_3\text{Sn}$  needles were located. Following the evolution of the dimensions of single needle in time, after the soldering process it was observed that the dimensions of the needle are increasing, and the maximum measured length was 14  $\mu\text{m}$ . If the increasing in length is about 8 times, the increasing in thickness is about 2.5 times, only. The needles start from 5-10  $\mu\text{m}$  from the  $\text{Cu}_3\text{Sn}$  border and they are oriented to the core of the solder.

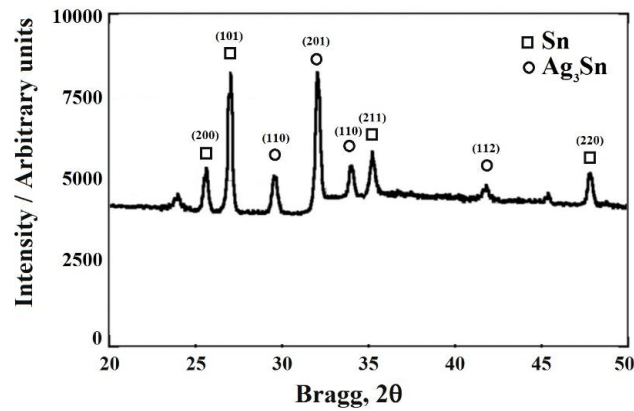
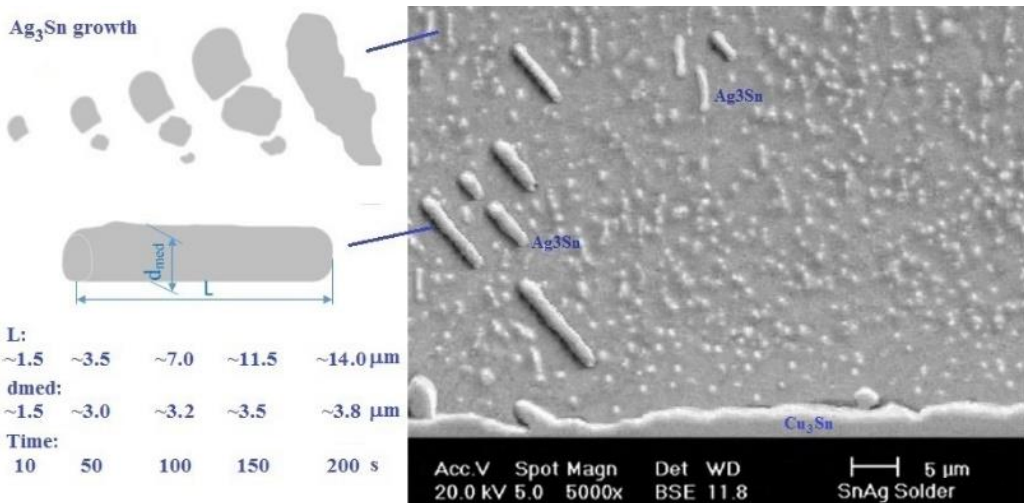


Fig. 11 XRD scattering of the deposited solder

Fig. 12 SEM image of the deposited solder and the observed evolution of the Ag<sub>3</sub>Sn IMC for classic resistive heating

Measuring the dimensions of the needles for up to 200 s period after the ending of the heating process, it was observed almost linear growth of the needles, in length. The thickness is increasing to double in the first 50 s and the growing is decreasing in speed after that value. The maximum thickness measured in SEM pictures was 3.8 μm. The application of the ultrasonic activation to the specimen B produced important agitation of the molten pool which is very clear visible on high speed video recordings of the process. The agitation results of inhibition of the nucleation of Ag<sub>3</sub>Sn IMC due to the continuous dispersion of the molten elements until the solidification of the solder. All the formed needles are grouped on specific areas, groups which are oriented to different directions starting from the Cu<sub>3</sub>Sn border to the core of the deposited solder.

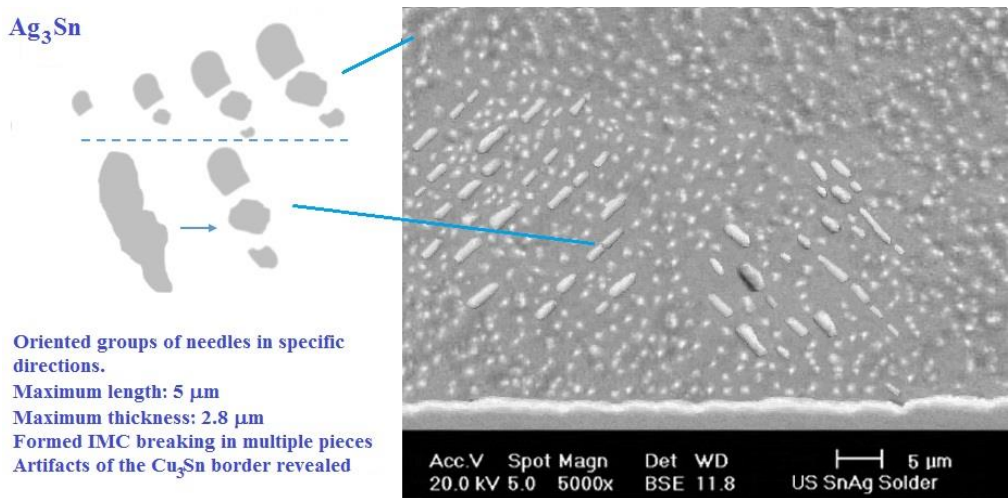


Fig. 13 SEM image of the deposited solder and the observed evolution of the  $\text{Ag}_3\text{Sn}$  IMC for hybrid resistive-ultrasonic heating

A second revealed phenomenon is that the nucleated  $\text{Ag}_3\text{Sn}$  IMCs are slowly and limited growing. Most of the grown needles are a third long comparing to the needles nucleated and grown during the classic heating cycle. A third phenomenon is related to cooling under vibration process and consists of the breaking of part of the formed needles. Not only the needles were proved to suffer breakings but the  $\text{Cu}_3\text{Sn}$  border revealed small artifacts broken at the edge. It can be observed in Fig. 13 (which was taken 24 h after the soldering process) that in the entire matrix of the deposited solder nucleation of the IMCs was happening. That means that the process of nucleation usually continues for several hours after the end of the soldering. In the same time, the growing of the needles depends on the dwelling time at specific temperature (Fig. 14).

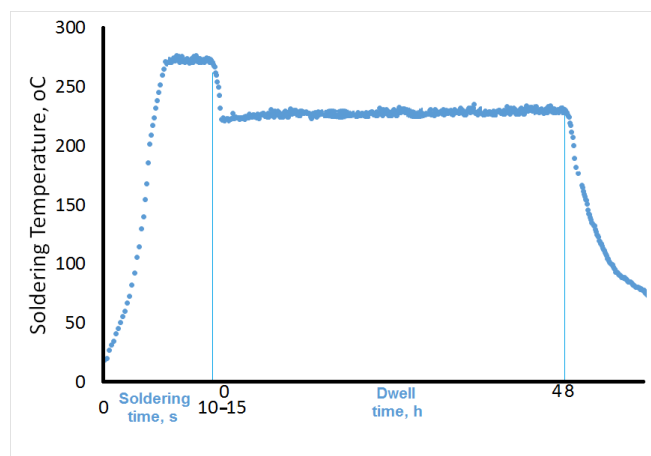


Fig. 14 Sketch of thermal cycle with dwell time after the soldering process

Fig. 15 shows the evolution of the  $\text{Ag}_3\text{Sn}$  needles for specimens A and Fig. 16 shows the evolution of the  $\text{Ag}_3\text{Sn}$  needles for specimens B.

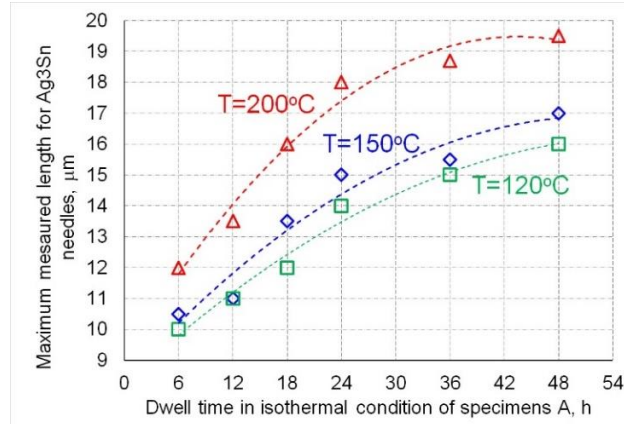


Fig. 15 Evolution of the  $\text{Ag}_3\text{Sn}$  needles for specimens A

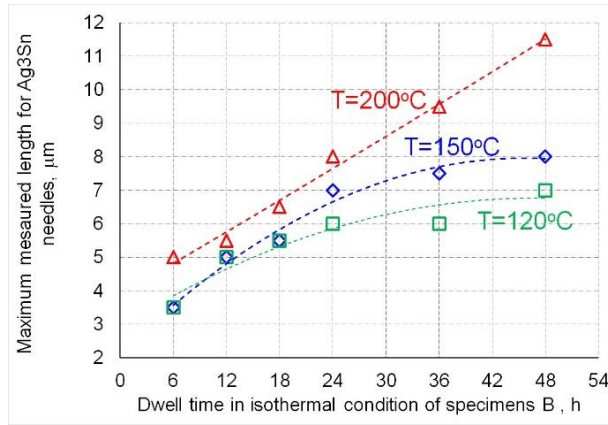


Fig. 16 Evolution of the  $\text{Ag}_3\text{Sn}$  needles for specimens B

Dwelling of the A-type and B-type specimens in isothermal conditions was assured for up to 48 hours, using 3 temperatures: 120°C, 150°C and 200°C. The measurements on SEM images revealed an increasing in length of the  $\text{Ag}_3\text{Sn}$  needles which remain oriented as after the soldering process and keep the initial orientation. If the limit between the tin matrix and the  $\text{Ag}_3\text{Sn}$  needles is very confusing after the soldering process, in 48 h of keeping at isothermal temperature the limit becomes clearer as visibility.

#### 4. Conclusions

Modelling of the wetting process using the input energies is possible by considering all the kinetic and potential energies which are acting at the solder surface layer.

If consider hybrid heat source which consists of resistive and ultrasonic distinct sources working in synergy conditions, then the energy to the surface is possible to be calculated. Better wetting will result for the hybrid heat source, so the energetic activation by using ultrasonic vibration improves the behavior of the solder during the soldering process.

The experiments revealed an increasing of 2.5 times of the wetting for the hybrid heating, important susceptibility to cracking for the classic resistive heating and tin dioxides on the surface of the both deposited solders. Inside the solder it has been revealed the existence of  $\text{Cu}_3\text{Sn}$  and  $\text{Ag}_3\text{Sn}$  intermetallic compounds, which start to nucleate and to grow-up inside the bond material.  $\text{Cu}_3\text{Sn}$  IMC nucleates in the very near vicinity of the solid-liquid interface and it forms a 3-6  $\mu\text{m}$  border along the interface.  $\text{Ag}_3\text{Sn}$  was revealed to have two types of shapes which appear on distinct cooling rates: flat islands in the matrix of  $\beta\text{-Sn}$  when the cooling rate is low and long needles when the cooling rate is high. The needles proved to have specific orientation from interface to the core of the solder.

The ultrasonic activation produced inhibition of the nucleation of  $\text{Ag}_3\text{Sn}$  IMC. The formed needles were broken by the vibration. By dwelling in isothermal conditions up to 48 h it has been observed that the needles are increasing in this period.

## R E F E R E N C E S

- [1]. *Abtew, M., Selvaduray, G.*, Lead-free Solder in Microelectronics, *Mater. Sci. Eng. R*, **vol.27**, 2000, 95-141.
- [2]. *Li, Y.-W., Lin, K.-L.*, Nucleation behaviors of the intermetallic compounds at the initial interfacial reaction between the liquid  $\text{Sn}3.0\text{Ag}0.5\text{Cu}$  solder and Ni substrate during reflow, *Intermetallics*, **vol. 32**, January 2013, 6–11
- [3]. *Kim, D. et. al.*, Formation and behavior of Kirkendall voids within intermetallic layers of solder joints, *Journal of Materials Science Materials in Electronics*, **vol. 22**, July 2011, 703-716
- [4]. *Han, Y.D., et al.*, Interfacial reaction and shear strength of Ni-coated carbon nanotubes reinforced Sn–Ag–Cu solder joints during thermal cycling, *Intermetallics*, **vol. 31**, December 2012, 72–78
- [5]. *Fürtauer, S., et.al.*, The Cu–Sn phase diagram, Part I: New experimental results, *Intermetallics*, **vol. 34**, March 2013, 142–147
- [6]. *Wang, C., Qin, F., An, T.*, Effects of IMC thickness on fracturing of solder joints, 11th Int. Conf. EPT&HDP, 2010, 511–514
- [7]. *Harris, P. G., Chaggar, K.S.*, Role of Intermetallic Compounds in Lead-free Soldering, *Soldering and Surface Mount Technology*, **vol. 10**, March 1998, 38-52
- [8]. *Fields, R. J., Low III, S. R., Lucey, G. K.*, Physical and mechanical properties of intermetallic compounds commonly found in solder joints, *Metal Science of Joining, Proceedings of TMS Symposium*, Cincinnati, October 1991, 20-24
- [9]. *R. Cabarat, L. Guillet, R. LeRoux*, The Elastic Properties of Metallic Alloys, *J. Inst. Metals*, **vol. 75**, 1949
- [10]. *Ostrovskaya, L.M., Rodin, V.N., Kuznetsov, A.I.*, Elastic Properties of Intermetallic Compounds Produced by Vacuum Deposition, *Soviet J. of Non-ferrous Metallurgy*, **vol.**

**26**, 1985

- [11]. *Lotfian, S.* et. al., Mechanical Characterization of Lead-Free Sn-Ag-Cu Solder Joints by High-Temperature Nanoindentation, *Journal of Electronic Materials*, **vol. 42**, June 2013, 1085–1091
- [12]. *Zhong, W.*, et. al., Mechanical properties of intermetallic compounds in solder joints, 11th Int. Conf. EPT&HDP, 2010, 520–524
- [13]. *Riggs, B.B.*, Thermodynamic and kinetic simulations of high temperature brazing: microstructure evolution in CMSX-4 joints, *Science and Technology of Welding&Joining*, November 2016, pp.1–10
- [14]. *Pongmorakot, K.*, et. al., Investigation on the mechanism of steel/steel solid-state bonding at low temperatures, *Science and Technology of Welding&Joining*, August 2016, 195–198
- [15]. *Liu, X.*, et. al, Effects of Ce addition on properties of Sn-0.3Ag-0.7Cu low-Ag lead-free solder, 11th Int. Conf. EPT&HDP, 2010, 176-180
- [16]. *Chen, C.-W.*, et.al. Current induced segregation of intermetallic compounds in three-dimensional integrated circuit microbumps, *Intermetallics*, **vol. 85**, June 2017, 117–124
- [17]. *Zhang, H.*, Effect of interlayer on microstructure and mechanical properties of Al-Ti ultrasonic welds, *Science and Technology of Welding&Joining* **vol. 22**, June 2016, 1-8
- [18]. *Schwartz, M.M.*, Soldering: Understanding the Basics, ASME International, 2014
- [19]. *Tsao, L.C.*, *Lo, T.T.*, *Peng, S.F.*, Growth kinetics of the intermetallic compounds during the interfacial reactions between Sn3.5Ag0.9Cu-nanoTiO<sub>2</sub> alloys and Cu substrate, 11th Int. Conf. EPT&HDP, 2010, 190-194
- [20]. *Rizvi, Y.C.*, *Bailey, C.*, *Lu, H.*, *Islam, M.N.*, Effect of Adding 1 wt% Bi into the Sn-2.8Ag-0.5Cu Solder Alloy on the Intermetallic Formations with Cu-Substrate During Soldering and Isothermal Aging, *J. Alloys and Compds.*, **vol. 407**, 2006, 208-214.,
- [21]. *Byron Jones, J.*, *Thomas, J.G.*, Ultrasonic Soldering of Aluminum, E.I. du Pont de Nemours & Company, Atomic Energy Division, Savannah River Laboratory, 1954
- [22]. *Walker, I.R.*, Reliability in Scientific Research: Improving the Dependability of Measurements, Calculations, Equipment, and Software, Cambridge University Press, 2011
- [23]. *Lujan-Facundo, M.J.*, et. al., Cleaning efficiency enhancement by ultrasounds for membranes used in dairy industries, *Ultrasonics Sonochemistry*, **vol. 33**, November 2016, 18–25
- [24]. *Galleguillos-Silva, R.*, *Vargas-Hernández, Y.*, *Gaete-Garretón, L.*, Wettability of a surface subjected to high frequency mechanical vibrations, *Ultrasonics Sonochemistry*, **vol. 35A**, March 2017, 134–141
- [25]. *Thangavadiel, K.*, et. al., Degradation of organic pollutants using ultrasound. In: *Chen D*, *Sharma SK*, *Mudhoo, A.*, Handbook on application of ultrasound: sonochemistry for sustainability. CRC Press, Taylor&Francis Group, Boca Raton, 2012
- [26]. *Osorio, W.R.*, *Garcia, A.*, Interrelation of wettability–microstructure–tensile strength of lead-free Sn–Ag and Sn–Bi solder alloys, *Science and Technology of Welding&Joining* **vol. 21**, March 2016, 1-9
- [27]. *Dogan, H.*, *Popov, V.*, Numerical simulation of the nonlinear ultrasonic pressure wave propagation in a cavitating bubbly liquid inside a sonochemical reactor, *Ultrasonics Sonochemistry*, **vol. 30**, May 2016, 87–97
- [28]. *Jian, Z.*, *Kuribayashi, K.*, *Jie, W.*, Solid-liquid interface energy of metals at melting point and undercooled state, *Materials Transactions*, **vol. 43**, 2002, 721-726
- [29]. *Zhou, M.-B.*, et. al., Interfacial reaction and melting/solidification characteristics between Sn and different metallizations of Cu,Ag,Ni and Co, 11th Int. Conf. EPT&HDP, 2010, 202–207
- [30]. *Liu, H.*, et. al., Comparative study of interfacial reactions of high-Sn Pb-free solders on (001) Ni single crystal and on polycrystalline Ni, 11th Int. Conf. EPT & HDP, 2010, 293–298

[31]. *Liu, L., Huang, M.*, Effect of solder volume on interfacial reactions between Sn3.5Ag0.75Cu solder balls and cu pad, 11<sup>th</sup>